



TECHNICAL UNIVERSITY OF CLUJ-NAPOCA

ACTA TECHNICA NAPOCENSIS

Series: Applied Mathematics, Mechanics, and Engineering  
Vol. 65, Issue Special IV, December, 2022

## AN OUTLOOK ON THE TRANSMISSION ERRORS OF NON-CIRCULAR GEARS DESIGNED BY SUPERSHAPE CENTRODE HYPOTHESIS

Mihai-Cătălin RADU, Paul-Adrian PASCU, Laurenția ANDREI, Gabriel ANDREI

**Abstract:** *The paper deals with both the generation and the transmission errors analysis for a specific non-circular gears train. Starting from one of the Gielis supershape as the driving gear pitch curve, an analytical procedure is applied to generate the mating gears teeth flanks. The simulation of meshing is further developed, introducing assembly errors for the gear mounting. The transmission errors are correlated with the variation of the centrodes curvature, offering information on the influence the modification of the gears pitch curve geometry, related to the assembly errors, has on the gears contact pattern. From the simulation performed, it was observed that meshing interval in ideal condition is greater compared to the case when the clearance is introduced.*

**Keywords:** *transmission error, gear meshing, tooth profile, gear misalignment, contact pattern.*

### 1. INTRODUCTION

In general, non-circular gears are used to make a shift from a constant speed input to a variable output speed or to use multiple-speed values that are constant at certain intervals during a rotation. One of the main benefits of non-circular gears is given by the variation of the transmission ratio; there are also other benefits of non-circular gears, in relation to other types of mechanisms, such as [1]: non-circular gears do not allow decoupling between elements, design of non-circular gears requires fewer components than camshafts, comparing to linkages, non-circular gears are well-balanced and more compact.

As regards the specific geometry and design procedure of the non-circular gears, with purely theoretical or applicative objectives, several attempts could be found in the literature. Danieli and Mundo [2] achieved the kinematic synthesis of a gear pair with a variable radius, starting from a predefined motion law. In order to simulate the orbit of the Moon and Mercury planet, Addomine et al. [3] presented the base elements of Dondi's astrarium which involve non-circular gear trains. Vasile and Andrei [4,5]

modeled non-circular gears using the equation of the super formula proposed by Gielis. Litvin [6] developed the non-circular gears generation process, based on the same tools that are used for the manufacture of cylindrical gears. Zheng et al. [7] provided a mathematical model for the variable center distance gear using the screw theory. Tsay and Fong [8] used an approach method of the Fourier series in order to approximate the pitch curve; the non-circular gear tooth profile was generated by a mathematical model that used the approximated pitch curve.

One of the main issues to be considered in mechanical transmissions is related to the presence of noise. Gear noise has three different elements: gear whine, gear clatter, and gear rattle.

Power transmission quality was first studied by Walker [9] who intended to reduce vibration and noise by analyzing the modifications of the spur gear tooth shape. Gear mesh tooth stiffness changes represent the cause for the appearance of the gear whine. Gear whine is a result of the static transmission error presence [10,11]. The existence of torsional oscillation generates both gear rattling and gear clattering [12]. The two

types of noises are different because gear clatter is generated by loaded gears and gear rattle represents a result of gear backlash.

Transmission error (TE) [13,14] represents the difference between the current location of the rotation angle of the output gear and the theoretical position when the gear mesh is completely conjugated. TE has four different parts: static transmission error (STE), dynamic transmission error (DTE), kinematic transmission error (KTE), and manufacturing transmission error (MTE). Transmission error is a result of manufacturing errors, shaft misalignment, tooth profile errors, tooth deflections, eccentricity, and dynamics of the gear. STE is a periodic function determined in the quasi-static regime. The noise magnitude base component is represented by the first harmonic of the mesh frequency. STE is also called loaded transmission error (LTE) [15]. The mathematical model and tooth contact analysis for non-circular gears was studied in Hang Xinghui et al. paper [16]. Jiang Han et al. [17] developed a non-circular gear transmission to obtain better accuracy and stability. The problem of unloaded transmission error for non-circular gears having misalignments was presented by Dooner and Mundo who also created a method to achieve the instantaneous gear ratio [18]. Fangyan Zheng et al. [19] proposed a new method for generating non-circular gears having a higher contact ratio and presenting the advantages of localized tooth contact.

In this paper, the meshing of a specific non-circular gear train is virtually analyzed to correlate the variation of the gears pitch curve's curvature radius with the contact pattern geometry and size, in case of induced assembly errors. For this purpose:

(i) A pair of non-circular gears is modelled based on the geometric hypothesis. The driving gear pitch curve is chosen as one of the Gielis' super shape, as the initial design data; a numerical procedure is developed to generate the conjugate pitch curve and teeth flanks profile, respectively, and specific codes and representations in AutoLISP and AutoCAD to enable the gears solid models to be produced;

(ii) The virtual non-circular gear pair is imported to Inventor and the gears mesh is analyzed considering ideal assembly features;

(iii) Center distance variation is introduced and the gears contact pattern is analyzed at moments when certain teeth pairs are in contact, respectively placed at the minimum and maximum gears pitch curves curvature.

## 2. GENERATION OF NON-CIRCULAR GEARS

In order to develop the proposed analysis on the non-circular gears transmission errors, a pair of gears are generated based on the geometric hypothesis, when the driving gear pitch curve is known. The traditional design algorithm requires (i) the driven curve geometry to be depicted and (ii) the gears teeth to be generated by either analytical procedure or simulation of gear manufacture.

### 2.1 Conjugated gears pitch curves generation

Using the hypothesis that the driving gear pitch curve is known, its geometry is chosen from the Gielis super shape family [20], defined by a multiparameter function:

$$r_{1(0)}(\varphi_1) = \left[ \left| \frac{1}{a} \cdot \cos \frac{n\varphi_1}{4} \right|^{n_2} + \left| \frac{1}{b} \cdot \sin \frac{n\varphi_1}{4} \right|^{n_3} \right]^{\frac{1}{n_1}} \quad (1)$$

where  $r_{1(0)}$ ,  $\varphi_1$  are the curve polar coordinates,  $\varphi_1 \in [0, 2\pi]$ ;  $a, b$  – the length of the super ellipse semi-axes (dimensionless),  $a, b \in \mathbb{R}_+^*$ ;  $n$  – parameter that induces the rotational symmetry for one rotation, if  $n \in \mathbb{Z}^*$ ;  $n_2, n_3$  – parameters that define if the curve is inscribed ( $n_2, n_3 < 2$ ) or circumscribed in the unit circle ( $n_2, n_3 > 2$ );  $n_1$  – parameter that introduces sharp/flatten corners and straight/convex/concave edges.

As the noncircular super shape is dimensionless, it will be further referred as the unit centrode, whose length is calculated as:

$$L_{1(0)} = \int_0^{2\pi} \sqrt{r_{1(0)}^2(\varphi_1) + \left( \frac{dr_{1(0)}}{d\varphi_1} \right)^2} d\varphi_1 \quad (2)$$

In order to insert the unit centrode into the gears theory, additional gears specific

parameters are defined, such as the gears modulus,  $m$ , and the number of teeth,  $z_1$ , respectively, and the unit centre is scaled to enable the gear teeth proper positioning, by ratio:

$$k_{sc} = \frac{\pi \cdot m \cdot z_1}{L_{1(0)}} \quad (3)$$

So, the noncircular gears design procedure will consider the pinion pitch curve being defined by:

$$r_1(\varphi_1) = k_{sc} \cdot r_{1(0)}(\varphi_1) \quad (4)$$

where  $\varphi_1$  is the pinion rotational angle,  $\varphi_1 \in [0, 2\pi]$ .

Following the mating centrodes generation algorithm [6], the driven gear pitch curve is defined by the equations:

$$\varphi_2(\varphi_1) = \int_0^{\varphi_1} \frac{r_1(\varphi_1)}{A - r_1(\varphi_1)} \cdot d\varphi_1 \quad (5)$$

$$r_2(\pi - \varphi_2(\varphi_1)) = A - r_1(\varphi_1) \quad (6)$$

where  $\varphi_2$  is the driven gear rotational angle,  $A$  – the gears center distance.

Equations (5), and (6) require the gears center distance,  $A$ , a parameter that is determined considering the rotational motions of conjugated gears during a period. In case the gear is rotated by  $\varphi_2 = 2\pi$  while the pinion also performs one rotation, the gears center distance should satisfy the equation:

$$2\pi = \int_0^{2\pi} \frac{r_1(\varphi_1)}{A - r_1(\varphi_1)} \cdot d\varphi_1 \quad (7)$$

### 2.2. Gears teeth generation

To generate the pinion section, an analytical procedure is combined with instruments of CAD application. The teeth active and inactive flanks are analytically expressed by the coordinates of flank points, the procedure considering the kinematics of the tooth flank cutting process when a standard rack-cutter tooth is involved. The pinion section is completed by editing the teeth roots in AutoCAD, by specified fillet radius.

In figure 1 it is shown the schematic representation of the pinion active tooth flank

generation; positioned by  $\varphi_{1i}$  polar angle ( $i = 1 \dots z_1$ ), related to the pinion pitch curve, the

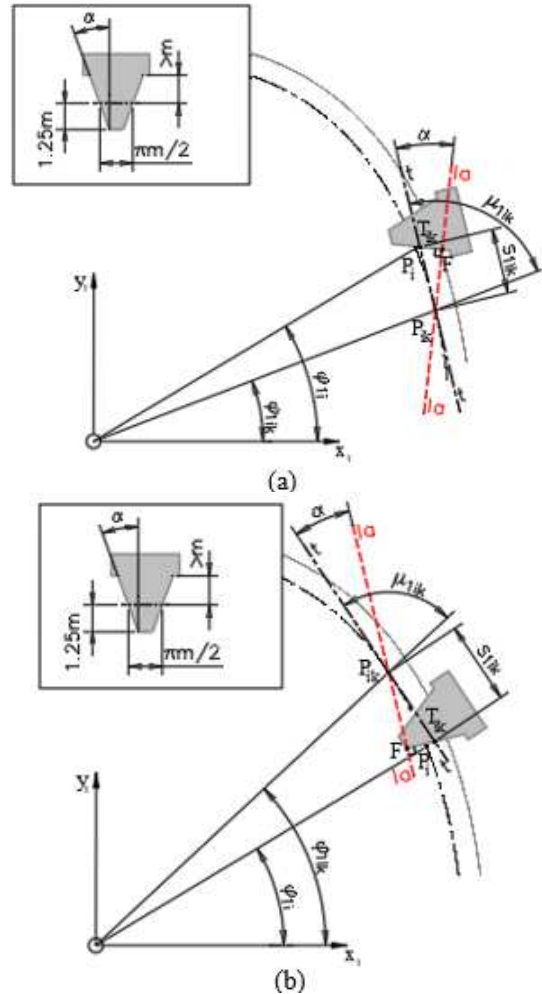


**Fig. 1.** Schematic representation of the active flank generation for tooth addendum (a) and tooth dedendum (b). (t) – the rack-cutter pitch line, (la) – the line of action, during the rolling motion;  $P_i$  – the tooth flank positioning point, relative to pitch curve;  $P_{ik}$  – the current point on the pinion pitch curve, during the rotational motion;  $T_{ik}$  – the point positioning the active rack-cutter flank, during translational motion;  $F$  – the generated tooth flank point

flank is generated by the pure rolling of the rack-cutter tooth, in the vicinity of the reference point  $P_i$ . At every instant,  $P_{ik}(\varphi_{1ik})$ , the rack-cutter pitch line inclination is modified, in order to remain tangent to the pinion pitch curve, and the rack-cutter tooth is translated by a distance ( $s_{1ik}$ ) that is in accordance with the pitch arc length ( $P_iP_{ik}$ ) during the pinion rotational motion. The generated tooth flank point,  $F_{ik}$ , is the intersecting point between the active rack-cutter flank and the line of action that remains

constantly inclined, by pressure angle  $\alpha$ , to the current rack-cutter pitch line.

The current geometry of the pinion active flank cutting process simulation enables the tooth flank points coordinates to be expressed as:

$$\begin{cases} x_{1F} = r_1(\varphi_{1ik}) \cdot \cos \varphi_{1ik} \pm s_{1ik} \cos \alpha \cdot \cos(\varphi_{1ik} + \mu_{1ik} - \alpha) \\ y_{1F} = r_1(\varphi_{1ik}) \cdot \sin \varphi_{1ik} \pm s_{1ik} \cos \alpha \cdot \sin(\varphi_{1ik} + \mu_{1ik} - \alpha) \end{cases} \quad (8)$$

where  $r_1$ ,  $\varphi_{1ik}$  are the polar coordinates of current point  $P_{ik}$  during the rolling motion, in the vicinity of reference point  $P_i$ ;  $s_{1ik}$  – the translation distance of the rack-cutter while the pinion is rotated by angle  $|\varphi_{1ik} - \varphi_{1i}|$ ;  $\alpha$  - the pressure angle;  $\mu_{1ik}$  – the inclination of the current tangent t-t, relative to the positioning vector of  $P_{ik}$  point, calculated by:

$$\mu_{1ik} = \arctan \left[ r_1(\varphi_{1ik}) \cdot \left( \frac{dr_1}{d\varphi_1}(\varphi_{1ik}) \right)^{-1} \right] \quad (9)$$

In equation (8), the (+) sign is for the tooth addendum flank coordinates calculation (figure 1a), while  $\varphi_{1ik} \in [\varphi_{1ia}, \varphi_{1i}]$ ; sign (-) is for the tooth dedendum flank coordinates calculation (figure 1b), while  $\varphi_{1ik} \in [\varphi_{1i}, \varphi_{1id}]$ . The angular limits for the pinion rotational motion,  $\varphi_{1ia}$ , and  $\varphi_{1id}$ , specific to the current flank ( $\varphi_{1i}$ ), are calculated from the equations:

$$\int_{\varphi_{1ia}}^{\varphi_{1i}} \sqrt{r_1^2(\varphi_1) + [r_1'(\varphi_1)]^2} d\varphi_1 = \frac{1,25m}{\sin \alpha \cdot \cos \alpha} \quad (10)$$

$$\int_{\varphi_{1i}}^{\varphi_{1id}} \sqrt{r_1^2(\varphi_1) + [r_1'(\varphi_1)]^2} d\varphi_1 = \frac{m}{\sin \alpha \cdot \cos \alpha} \quad (11)$$

A similar schematic geometry is considered for the tooth inactive flank generation, positioned by  $P_i'$ , leading to the following expressions:

$$\begin{cases} x_{1F'} = r_1(\varphi_{1ij}) \cdot \cos \varphi_{1ij} \mp s_{1ij} \cos \alpha \cdot \cos(\varphi_{1ij} + \mu_{1ij} + \alpha) \\ y_{1F'} = r_1(\varphi_{1ij}) \cdot \sin \varphi_{1ij} \mp s_{1ij} \cos \alpha \cdot \sin(\varphi_{1ij} + \mu_{1ij} + \alpha) \end{cases} \quad (12)$$

where  $r_1$ ,  $\varphi_{1ij}$  are the polar coordinates of the current point during the rolling motion, in the vicinity of the reference point  $P_i'$ , that is positioning the inactive flank;  $s_{1ij}$  – the translation distance of the rack-cutter while the pinion is rotated by angle  $|\varphi_{1ij} - \varphi_{1i}|$ ;  $\alpha$  - the pressure

angle;  $\mu_{1ij}$  – the inclination of current tangent t-t, relative to the positioning vector of  $P_i'$  point.

Using coordinate transformations, the driven gear tooth flanks, as conjugate flanks of the pinion teeth flanks, are described by [21]:

$$\begin{cases} x_2(\varphi_2) = -A \cdot \cos \varphi_2 + x_1(\varphi_1) \cdot \cos(\varphi_1 + \varphi_2) + y_1(\varphi_1) \cdot \sin(\varphi_1 + \varphi_2) \\ y_2(\varphi_2) = A \cdot \sin \varphi_2 - x_1(\varphi_1) \cdot \sin(\varphi_1 + \varphi_2) + y_1(\varphi_1) \cdot \cos(\varphi_1 + \varphi_2) \end{cases} \quad (13)$$

where  $\varphi_1$  is the current polar angle of the pinion tooth flank generated point;  $x_1$ ,  $y_1$  – the coordinates of the pinion tooth flank generated point, from equations (8), (12);  $\varphi_2$  – the corresponding driven gear rotational angle, calculated by equation (5).

To get the non-circular pinion and gear solid models, the database is further imported to AutoCAD wherein the gears sections profiles are edited by filleting the teeth roots and extruded by the desired gear face width.

### 3. INFLUENCE OF TRANSMISSION ERRORS ON NON-CIRCULAR GEARS CONTACT PATTERN

First, the non-circular gears were studied in the ideal condition with no geometric or assembly errors.

Then, to determine how the transmission error function affects the geometry of the contact pattern when alignment errors occur, the relative location of the wheel with regard to the pinion is established.

The alignment error studied in this paper is the clearance.

This was obtained with the increase of the center distance ( $\Delta A$ ) as shown in figure 2.

During meshing, the contact pattern offers qualitative data on the geometry of the contact line and the surface on which the load is distributed.

When clearance is taken into consideration, the theoretical contact line of the tooth contact pair changes.

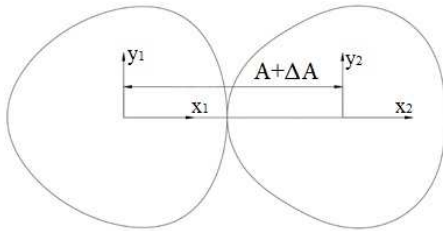


Fig. 2. Center distance error alignment

#### 4. NUMERICAL RESULTS

In order to develop the influence of the pitch curve radius/curvature on the gears transmission radius, a pair of non-circular gears are generated based on the pinion pitch curve geometry, as initial data. Although equation (1) enables unlimited variable super shape geometries, it is obvious that not all of them could be considered as gear pitch curves. Therefore, to simplify the curve geometry and to avoid undercutting during the teeth generation process, the super shape's defining parameters are chosen to lead to a closed symmetrical gear centrod, with no sharp corners and no concave edges. In figure 3 are illustrated the unit centrod/super shape, defined by the parameters  $a = b = 1$ ,  $n = 3$ ,  $n_1 = 6$ ,  $n_2 = n_3 = 4$  and the pinion pitch curve, as the scaled unit centrod, corresponding to gears defining parameters:  $m = 3$  mm,  $z_1 = 36$ . Figure 4 illustrates the pinion and gear pitch curves; choosing the driven gear number of teeth  $z_2 = z_1$ , the center distance is calculated from equation (7) as  $A = 107,365$  mm.

AutoLISP codes are created to enable the generation of teeth active and inactive flanks, for both pinion and gear, in AutoCAD environment, using equations (8), (12), and (13) and considering the pressure angle at the standard constant value of  $20^\circ$ . The flank profiles are generated as polylines, with 400 vertices, within their individual generating angular limits, defining the units precision, for both length and angle, as  $10^{-8}^\circ$  (figure 5). The designed gears sections geometry is further completed by introducing the dedendum circle, which offsets the pitch curve at a distance of  $1,25m$ , and filleting it with the teeth flanks profiles by a radius of  $0,25m$ . To generate the gears solid models, the gears face width is considered as  $B = 36$  mm (figure 6).

#### 4.1. Contact pattern analysis

The contact pattern is influenced by the direction of the transmitted torque and the position of the wheels on the shafts. The geometry of the contact pattern is determined from the virtual model of the non-circular gears analyzed in Autodesk Inventor.

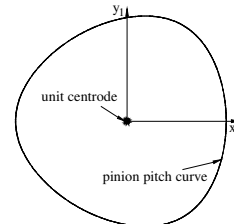


Fig. 3. Pinion unit centrod and pitch curve for  $a = b = 1$ ,  $n = 3$ ,  $n_1 = 6$ ,  $n_2 = n_3 = 4$ ,  $m = 3$  mm,  $z_1 = 36$ .

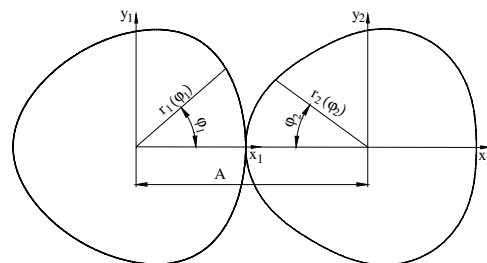


Fig. 4. Non-circular mating pitch curves for a gear train defined by  $m = 3$  mm,  $z_1 = z_2 = 36$ .

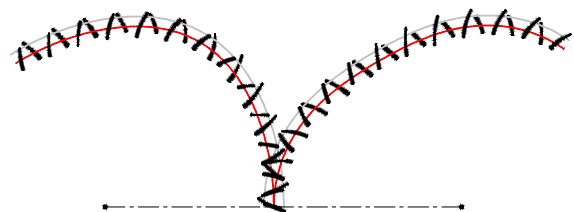


Fig. 5. Gears teeth flanks profiles along one gears lobe.

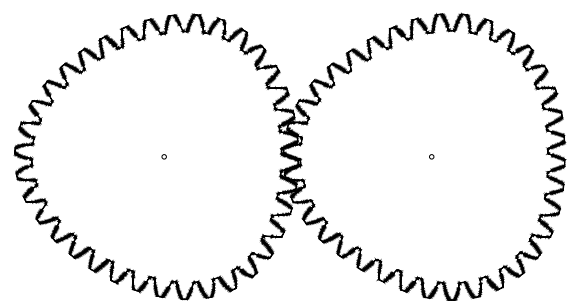
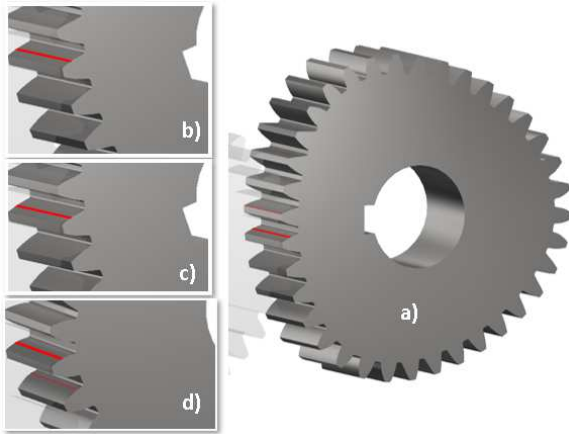


Fig. 6. Sections of designed non-circular gears, with root fillet

Figure 7 presents the modification of the contact pattern geometry obtained through solid modeling, analyzed from a kinematic point of view and in ideal conditions. The contact between

the tooth flank was obtained by introducing an interference of 0.07 mm. The form of the contact pattern is determined through manual incrementing. Due to the symmetry of rotation, in



**Fig. 7.** Contact pattern geometry in ideal condition: a) beginning of meshing, b) rotation by 19.2°, c) rotation by 60.1°, d) rotation by 78.5°

It can be seen that the meshing interval for the first tooth that comes into contact at the base of one lobe is 19.2 degrees. The meshing interval for the tooth that comes in contact near the axis of the lobe is 18.5 degrees. There are two teeth in meshing except in two small regions where only one tooth mesh.

The contact pattern for the model that was developed with radial clearance is shown in figure 8 and figure 9. There are 2 situations: first with a 0.5mm clearance, and the second with a 1mm clearance.

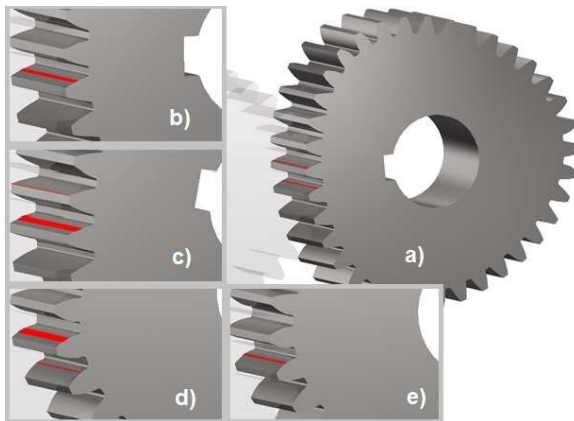


**Fig. 8.** Contact pattern geometry with 0.5mm clearance: a) beginning of meshing, b) rotation by 4°, c) rotation by 15.3°, d) rotation by 56°; e) rotation by 63°

the example consider, the pitch curve has 3 lobes with a symmetrical configuration with respect to the "axis" of the lobe.

Analyzing the contact pattern when clearance is taken into account, it can be observed that the meshing interval is decreasing by 4 degrees. Usually, two teeth are in mesh.

It can also be seen that interference occurs between the meshing teeth, usually after a rotation of about 7 degrees from the beginning of the meshing.

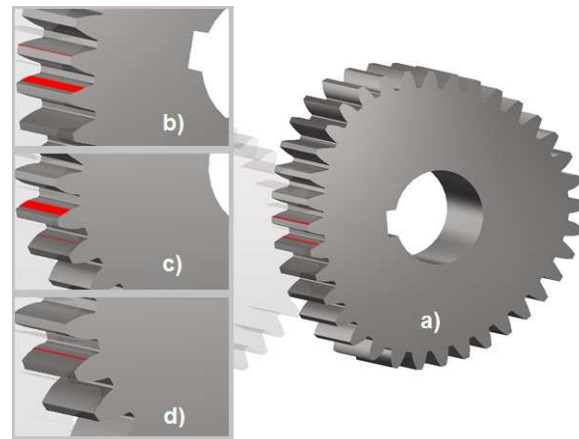


**Fig. 9.** Contact pattern geometry with 1mm clearance: a) beginning of meshing, b) rotation by 15.1°, c) rotation by 56°; d) rotation by 63.2°

## 5. CONCLUSIONS

In this paper, the meshing of a specific non-circular gear train is virtually analyzed to correlate the variation of the gears pitch curve's curvature radius with the contact pattern geometry and size, in case of induced assembly errors.

A pair of non-circular gears is modelled based on the geometric hypothesis. The driving gear pitch curve is chosen as one of Gielis' super shape. The virtual non-circular gear pair is imported to Inventor and the gear mesh is analyzed considering ideal assembly features and when center distance variation is introduced. The alignment error studied in this paper is the clearance. The modification of the contact pattern geometry is obtained through solid modeling and analyzed from a kinematic point of view, in ideal conditions and also when

clearance is induced. The form of the contact pattern is determined through manual incrementing.

It was observed through the simulation that the meshing interval is longer under ideal conditions than it is when the clearance is present. Both in the ideal case and in the case when clearance is considered, the meshing is obtained with two pairs of teeth, except for a small interval of approximately 2 degrees where only one pair of teeth is in meshing.

## 6. REFERENCES

- [1] Dooner D. B., Seireg A. *The kinematic geometry of gearing*. John Wiley & Sons, ISBN 0-471-04597-7, New York, 1995, <https://doi.org/10.1002/9781119942474>
- [2] Danieli, G.A., Mundo, D. *New developments in variable radius gears using constant pressure angle teeth*. Mech Mach Theory 40, 203-17, 2005, <https://doi.org/10.1016/j.mechmachtheory.2004.06.005>
- [3] Addomine, M., Figliolini, G., Pennestrì E. *A landmark in the history of non-circular gears design: The mechanical masterpiece of Dondi's astrarium*, Mech Mach Theory 122, 219-232, 2018, <https://doi.org/10.1016/j.mechmachtheory.2017.12.027>
- [4] Vasie, M., Andrei, L. *Noncircular gear design and generation by rack cutter*. The Annals of "Dunarea de Jos University of Galati", Fasc. V, Technologies in Machine Building, 81-86, 2011.
- [5] Vasie, M., Andrei, L. *Analysis of Noncircular gear meshing*. Mechanical Testing and Diagnosis 4, 70-78, 2012.
- [6] Litvin, F. L., Gonzalez-Perez, I., Fuentes, A., Hayasaka, K. *Design and investigation of gear drives with non-circular gears applied for speed variation and generation of functions*. Comput Methods Appl Mech Eng, 197, 3783–802, 2008, <https://doi.org/10.1016/j.cma.2008.03.001>
- [7] Zheng, F., Hua, L., Han, X. *The mathematical model and mechanical properties of variable center distance gears based on screw theory*. Mech Mach Theory, 101, 116–39, 2016, <https://doi.org/10.1016/j.mechmachtheory.2016.03.005>
- [8] Tsay, M-F., Fong, Z-H. *Study on the generalized mathematical model of non-circular gears*. Math Comput Model, 41, 555-69, 2005, <https://doi.org/10.1016/j.mcm.2003.08.010>
- [9] Walker, H. *Gear Tooth Deflection and Profile Modification*, Engineer 166, 410-35, 1938, [https://doi.org/10.1007/978-0-387-92897-5\\_573](https://doi.org/10.1007/978-0-387-92897-5_573)
- [10] Gregory, R. W., Harris, S. L., Munro, R. G. *Dynamic behaviour of spur gears*, Proc Inst Mech Eng, 178, 207-18, 1963, <https://doi.org/10.1177/002034836317800130>
- [11] Welbourn, D. B. *Fundamental Knowledge of Gear Noise*. Conference on noise and vibrations of engines and transmission, Cranfield Institute of Technology, paper C117/79, 9-29 (1979).
- [12] Fietkau, P., Bertsche. B. *Influence of tribological and geometrical parameters on lubrication conditions and noise of gear transmissions*. Mech Mach Theory, 69, 303–20, 2013, <https://doi.org/10.1016/j.mechmachtheory.2013.06.007>
- [13] Garambois, P., Perret-Liaudet, J., Rigaud, E. *NVH robust optimization of gear macro and microgeometries using an efficient tooth contact model*. Mech Mach Theory, 117, 78–95, 2017, <https://doi.org/10.1016/j.mechmachtheory.2017.07.008>
- [14] Gregory, R.W, Harris, S.L., Munro, R.G. *A Method of Measuring Transmission Error in Spur Gears of 1:1 Ratio*. J Sci Instrum, 40, 5-9, 1963, <https://doi.org/10.1088/0950-7671/40/1/303>
- [15] Fernandez del Rincon, A., Viadero, F., Iglesias, M., García, P., de-Juan A., Sancibrian R. *A model for the study of meshing stiffness in spur gear transmissions*. Mech Mach Theory 61, 30–58, 2013, <https://doi.org/10.1016/j.mechmachtheory.2012.10.008>
- [16] Han, X.-H., Zhang, X.-C., Zheng, F.-Y., XU, M., Tian J. *Mathematic model and tooth contact analysis of a new spiral non-circular bevel gear*. J Cent South Univ, 29, 157 – 72, 2022, <https://doi.org/10.1007/s11771-022-4898-8>
- [17] Jiang, H., Dazhu, L., Xiaoqing, T., Lian, X. *Meshing principle and transmission analysis of a beveloid non-circular gear*, Adv Mech Eng 12(11), 1–11, 2020, <https://doi.org/10.1177/1687814020971909>

- [18] Dooner, D., Mundo, D. *Unloaded transmission error and instantaneous gear ratio for non-circular gears with misalignments*. Mech Mach Theory 170, 104728, 2022, <https://doi.org/10.1016/j.mechmachtheory.2022.104728>
- [19] Fangyan, Z., Han, X., Lin, H., Mingde, Z., Weiqing, Z. *Design and manufacture of new type of non-circular cylindrical gear generated by face-milling method*, Mech Mach Theory, 122, 326-346, 2018, <https://doi.org/10.1016/j.mechmachtheory.2018.01.007>
- [20] Gielis, J., Beirinckx, B., Bastiaens, E. *Superquadrics with rational and irrational symmetry*. Proc. of the 8<sup>th</sup> ACM Symposium on Solid Modeling & Applications, 262-265, June, 2003, <https://doi.org/10.1145/781606.781647>
- [21] Niculescu, M., Andrei, L., Cristescu, A. *Generation of noncircular gears for variable motion of the crank-slider mechanism*. IOP Conf Ser: Mater Sci Eng, 147, 012078, 2016, <https://doi.org/10.1088/1757-899X/147/1/012078>

### O PERSPECTIVĂ PRIVIND ERORILE DE TRANSMITERE ALE ROȚILOR DINȚATE NECIRCULARE PROIECTATE PRIN INTERMEDIUL IPOTEZEI CENTROIDEI SUPERFORMEI

Lucrarea tratează atât generarea angrenajelor necirculare, cât și analiza erorilor de transmitere pentru un anumit tip de angrenaj necircular. Având ca punct de plecare una dintre superformele propuse de Gielis pentru curba de divizare a pinionului, o procedură analitică este aplicată pentru a genera flancurile dinților roților conjugate. Simularea angrenării este evidențiată apoi prin introducerea erorilor de asamblare. Erorile de transmitere sunt corelate cu variația curburii centroidelor, oferind informații despre influența pe care modificarea geometriei curbei de divizare a roților, în raport cu erorile de asamblare, o are asupra petei de contact. Din simularile realizate s-a constatat că intervalul de angrenare în condiții ideale este mai mare comparativ cu situația în care se introduce jocul la piciorul dintelui.

**Mihai-Cătălin RADU**, Drd. Ing, Assistant, University Dunarea de Jos of Galati, Faculty of Engineering, Mechanical Engineering Department, [radumihaicat@gmail.com](mailto:radumihaicat@gmail.com), 0734584430.

**Paul-Adrian PASCU**, Drd. Ing, University Dunarea de Jos of Galati, Faculty of Engineering, Mechanical Engineering Department, [pascu.pauladrian@yahoo.com](mailto:pascu.pauladrian@yahoo.com).

**Laurenția ANDREI**, Dr. Ing, Professor, University Dunarea de Jos of Galati, Faculty of Engineering, Mechanical Engineering Department, [Laurencia.Andrei@ugal.ro](mailto:Laurencia.Andrei@ugal.ro).

**Gabriel ANDREI**, Dr. Ing, Professor, University Dunarea de Jos of Galati, Faculty of Engineering, Mechanical Engineering Department, [Gabriel.Andrei@ugal.ro](mailto:Gabriel.Andrei@ugal.ro).